

Examining Natural Attenuation and Acute Toxicity of Petroleum-Derived Dissolved Organic Matter with Optical Spectroscopy

David C. Podgorski,^{*,†,Ⓛ} Phoebe Zito,[†] Jennifer T. McGuire,[‡] Dalma Martinovic-Weigelt,[‡] Isabelle M. Cozzarelli,^{§,Ⓛ} Barbara A. Bekins,^{||} and Robert G. M. Spencer[⊥]

[†]Pontchartrain Institute for Environmental Sciences, Department of Chemistry, University of New Orleans, New Orleans, Louisiana 70148, United States

[‡]Department of Biology, University of St. Thomas, St. Paul, Minnesota 55105, United States

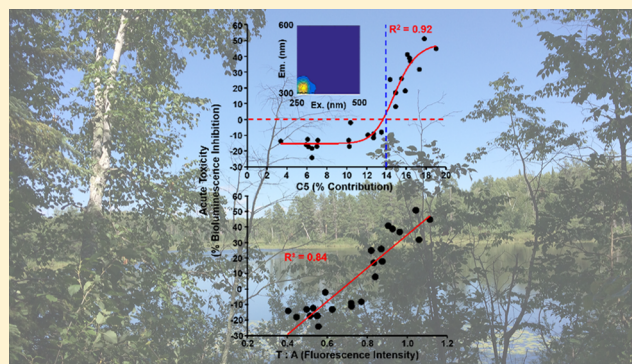
[§]U.S. Geological Survey, Reston, Virginia 20192, United States

^{||}U.S. Geological Survey, Menlo Park, California 94025, United States

[⊥]Department of Earth, Ocean and Atmospheric Science, Florida State University, Tallahassee, Florida 32306, United States

Supporting Information

ABSTRACT: Groundwater samples containing petroleum-derived dissolved organic matter (DOM_{HC}) originating from the north oil body within the National Crude Oil Spill Fate and Natural Attenuation Research Site near Bemidji, MN, USA were analyzed by optical spectroscopic techniques (i.e., absorbance and fluorescence) to assess relationships that can be used to examine natural attenuation and toxicity of DOM_{HC} in contaminated groundwater. A strong correlation between the concentration of dissolved organic carbon (DOC) and absorbance at 254 nm (a_{254}) along a transect of the DOM_{HC} plume indicates that a_{254} can be used to quantitatively assess natural attenuation of DOM_{HC}. Fluorescence components, identified by parallel factor (PARAFAC) analysis, show that the composition of the DOM_{HC} beneath and adjacent to the oil body is dominated by aliphatic, low O/C compounds (“protein-like” fluorescence) and that the composition gradually evolves to aromatic, high O/C compounds (“humic-/fulvic-like” fluorescence) as a function of distance downgradient from the oil body. Finally, a direct, positive correlation between optical properties and Microtox acute toxicity assays demonstrates the utility of these combined techniques in assessing the spatial and temporal natural attenuation and toxicity of the DOM_{HC} in petroleum-impacted groundwater systems.



1. INTRODUCTION

Crude oil is a complex mixture of naturally occurring organic matter predominately composed of hydrocarbons (HC), with minor contributions from nitrogen, sulfur, oxygen, and trace metals. Once released to the surface from the Earth’s interior, oxygenation by microbial and photochemical processes results in the formation of oxyhydrocarbons (HC_{oxy}).¹ Though photochemical degradation processes produce HC_{oxy} in oxic environments by reacting with aromatic compounds that absorb light in the solar spectrum, microbes can also transform aliphatic and light aromatic fractions to HC_{oxy} by both aerobic and anaerobic degradation processes.^{2–6} Changes in solubility that coincide with the transformation of HC to HC_{oxy}, by both photochemical and microbial processes, can result in the production of petroleum-derived dissolved organic matter (DOM_{HC}).^{7–9} Potentially toxic HC_{oxy} may be distributed throughout aquatic environments once mobilized by dissolution, impacting aquatic ecosystems and drinking water supplies.^{10–12} The development of cost-efficient and robust methods to examine the composition and movement of

DOM_{HC} is critical for determining how these compounds migrate and their ultimate fate in the environment.

The quantity of dissolved organic carbon (DOC) and quality of dissolved organic matter (DOM) can be investigated by analyzing the properties of chromophoric dissolved organic matter (CDOM), the light absorbing fraction of DOM, via optical measurements (i.e., absorbance and fluorescence spectroscopy).^{13–19} Relationships between CDOM parameters and DOM molecular weight, aromaticity, source, and reactivity have been extensively documented in recent years.^{20–28} In addition, fluorescence components, identified by parallel factor (PARAFAC) analysis of excitation–emission matrices (EEMs), can provide detailed information about DOM quality.^{29–33} Although studies report the properties of petroleum-derived CDOM (CDOM_{HC}) in marine and groundwater systems, little

Received: January 2, 2018

Revised: April 6, 2018

Accepted: May 1, 2018

Published: May 1, 2018

is known about how changes in $CDOM_{HC}$ correlate with DOM_{HC} concentration, natural attenuation, biodegradation, and toxicity.^{34–39}

Aquatic ecosystems are particularly susceptible to contamination from DOM_{HC} that can be readily transported through water movement (e.g., in fluvial networks and between groundwater and surface waters). Tracking the migration, concentration, chemical composition, and potential toxicity of these complex mixtures is critical for making both short- and long-term spill-response decisions. Postspill, long-term observations are required to determine the fate of the oil, and degradation products, in the surrounding environment. Optical spectroscopy has been utilized for many years to detect and monitor oil in aquatic ecosystems. Applications include estimating petroleum residue concentrations, fingerprinting of chemically dispersed oil in water, detecting and monitoring of surface oil slicks, determining oil droplet sizes, and estimating the concentration of benzene, toluene, ethylbenzene, and xylene (BTEX) and total petroleum hydrocarbons (TPH).^{40–45} This study investigates the utility of optical spectroscopic measurements for the detection and examination of $CDOM_{HC}$ in DOM_{HC} impacted groundwater. The work builds on previous characterization of DOM and oil spill detection and monitoring by showing the application of optical spectroscopy to (1) measure rates of natural attenuation of DOM_{HC} in a groundwater plume; (2) determine changes in chemical composition of DOM_{HC} from biodegradation; and (3) characterize relationships between chemical composition of DOM_{HC} and acute toxicity. We hypothesized that, although the composition of $CDOM_{HC}$ becomes increasingly similar to that observed in the native groundwater because of biodegradation, the $CDOM_{HC}$ will retain a unique optical signature detectable in groundwater hundreds of meters from the petroleum source. Moreover, we hypothesized that specific components of $CDOM_{HC}$ are potential indicators of toxic DOM_{HC} mixtures in aquatic environments. We tested these hypotheses by measuring the optical properties and screening acute toxicity of a DOM_{HC} plume origination from a subsurface oil body that has been present in an aquifer for nearly 40 years.

2. MATERIALS AND METHODS

2.1. Site Description and Sample Collection. An oil pipeline rupture in 1979 located outside the city of Bemidji, MN (USA) sprayed approximately 1.7 million L of light (33° API) crude oil across an area of 6500 m².⁷ The spilled oil contained 0.56% sulfur and 0.28% nitrogen with a composition of 58–61% saturated hydrocarbons, 33–35% aromatics, 4–6% resins, and 1–2% asphaltenes.⁴⁶ The oil subsequently collected into depressions and approximately 25% of the unrecovered oil percolated through silt, sand, gravel, and glacial till to form three residual oil bodies at the water table of the underlying aquifer.⁹ Samples from 32 wells were collected in the summer of 2016 from the north oil pool where the water table is 6–8 m below the land surface and the groundwater flows east-northeast at an average velocity of 22 m yr⁻¹ toward the Unnamed Lake.⁷ Detailed maps and descriptions of the sample site are elsewhere.^{7,9,46–48} Each well was purged with at least three-well volumes and samples were not collected until field measurements of pH, dissolved oxygen, temperature, and specific conductance stabilized. A database of the field measurements can be found at <https://mn.water.usgs.gov/projects/bemidji/>. The terms natural attenuation and biode-

gradation are used interchangeably from this point forward because biodegradation is the main process at the site.

2.2. Dissolved Organic Carbon (DOC) Analyses. Each water sample was filtered through a precleaned 0.2 μm Supor filter into a precombusted (550 °C > 5 h) amber glass vial. The pH of each sample was immediately adjusted with hydrochloric acid to pH < 2 and samples were stored in the dark and refrigerated (<4 °C) until subsequent DOC analysis. Dissolved organic carbon measurements were completed by the high temperature combustion technique with a Shimadzu TOC Vcsm analyzer using previously described methods.^{9,49} DOC data are the mean of three to six replicate injections for which the coefficient of variance was less than 2%. In this manuscript, the term DOC is equivalent to nonvolatile dissolved organic carbon (NVDOC) used in previous studies at the Bemidji site.^{9,46–48}

2.3. Optical Analyses. Each sample was filtered through a precombusted (450 °C > 5 h) Advantec GF-75 0.3 μm glass fiber-filter prior to pH adjustment (pH 8) for absorbance and fluorescence measurements with an Aqualog fluorometer (Horiba Scientific, Kyoto, Japan).^{50–52} Measurements were completed in a 10 mm quartz cuvette at a constant temperature of 20 °C. Absorbance and excitation scans were collected from 240–800 nm in 5 nm increments with an integration period of 0.5 s. Milli-Q water (18.2 M Ω cm⁻¹) was used to dilute each sample to an absorbance of 0.1 at 254 nm to reduce inner filter effects.^{23,53} Spectra were blank subtracted and corrected for instrument bias in excitation and emission prior to correction for inner filter effects. Fluorescence intensities were normalized to Raman scattering units and dilution corrected prior to Parallel Factor (PARAFAC) analysis. PARAFAC is a multiway data analysis method that is used to decompose fluorescence excitation–emission matrix (EEM) spectra into underlying spectral properties.⁵⁴ PARAFAC of EEM spectra obtained for 129 DOM_{HC} were used to develop the model with the drEEM toolbox (tutorial and MatLab code).⁵⁴ With the exception of the background wells (310 B and 310 E) all of the samples used for the PARAFAC model contained DOM_{HC} . The spectral properties for each of the six components were examined and then validated by residual and split-half analysis.^{55,56} The relative contributions of C1–C6 were determined by summing the model scores. Figures 1 and S1 show the spectral properties for components 1–6. The components from this PARAFAC model were matched to others reported in the OpenFluor database that have a Tucker's congruence coefficient threshold of 0.95 for an identical match between spectra.⁵⁷ The humification index (HIX) was determined by the area under the emission spectra between 435 and 480 nm divided by the sum of the peak areas from 300 to 345 nm and 435 to 480 nm.²³

2.4. Microtox Screening. The water samples were assessed for acute toxicity ($N = 30$; Microtox, Modern Water, Guildford, UK). This *Vibrio fischeri* bioluminescence inhibition assay was selected because its effect concentrations are correlated to other aquatic toxicity end points,⁵⁸ and it is suitable for toxic equivalency evaluation of complex environmental samples including groundwater where it has been shown to correlate well with the in vivo *Daphnia magna* toxicity assays.⁵⁹ Raw, unfiltered water samples were first allowed to settle; the resulting supernatant was transferred to a glass vial, enriched with the osmotic adjusting solution (sodium chloride solution that brings salinity of the samples to approximately 2%), and analyzed within minutes of the sample collection. Light loss or

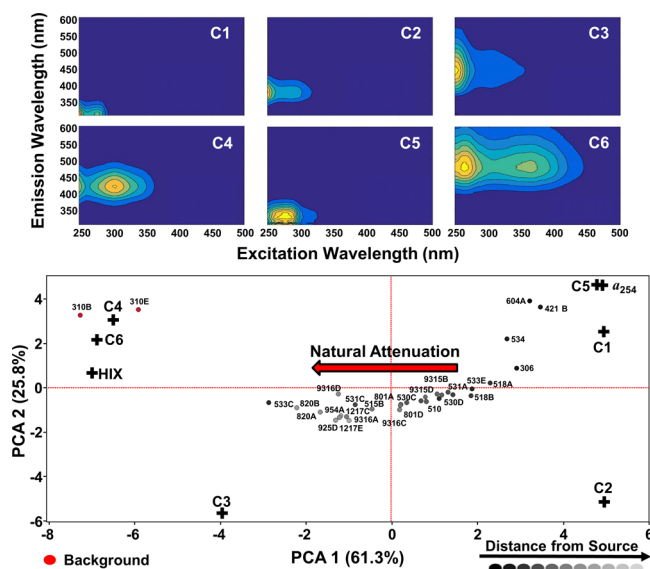


Figure 1. Six components obtained from the validated PARAFAC model (top). Principal component analysis (PCA) of the values obtained by optical measurements of the DOM_{HC} at the Bemidji Site (bottom).

gain in the samples relative to a control sample (reagent blank provided by the manufacturer) was calculated. All measurements and data analyses were performed following manufacturer's protocols for B-Tox Test procedure using Deltatox II photometer (Modern Water).

3. RESULTS AND DISCUSSION

3.1. Degradation of Petroleum-Derived Dissolved Organic Carbon.

The north oil pool at the Bemidji site is a source of carbon for the DOC plume that extends in excess of 325 m downgradient prior to reaching the shore of the Unnamed Lake.⁹ The DOC concentrations measured at each sampled well versus the distance from the center of the oil body are shown in Figure 2a and Table S1. Well 518A, the well nearest to the center of the oil body (~57 m), contains groundwater with a DOC concentration of 31.1 mg L^{-1} . Approximately 200 m downgradient from well 518A, the DOC concentration is over an order of magnitude less (Figure 2a). This exponential decay of DOC concentration (measured in each well that transects the plume originating from the north oil body) shows the natural attenuation of petroleum-derived DOC (DOC_{HC}) at the Bemidji site and corroborates previous reports of a first-order degradation rate of $\sim 0.13\% \text{ d}^{-1}$.⁶⁰ Equation 1 describes the natural attenuation of DOC_{HC} originating from the north oil pool in this study. Here, y is the modeled DOC_{HC} concentration at a given time. The y_0 term is the predicted stable DOC_{HC} concentration. The value calculated for the A term describes the initial DOC_{HC} concentration. Finally, τ is a time constant and x is the residence time of the DOC_{HC} in the aquifer. The value for each term is determined by utilizing the known distance from the center of the oil body for each well in combination with the mean flow velocity of the groundwater in the aquifer of 0.06 m d^{-1} (21.9 m yr^{-1}).^{7,61}

$$y = y_0 + Ae^{x/\tau} \quad (1)$$

The ability to fit the natural attenuation of DOC_{HC} to an exponential decay curve provides a wealth of information

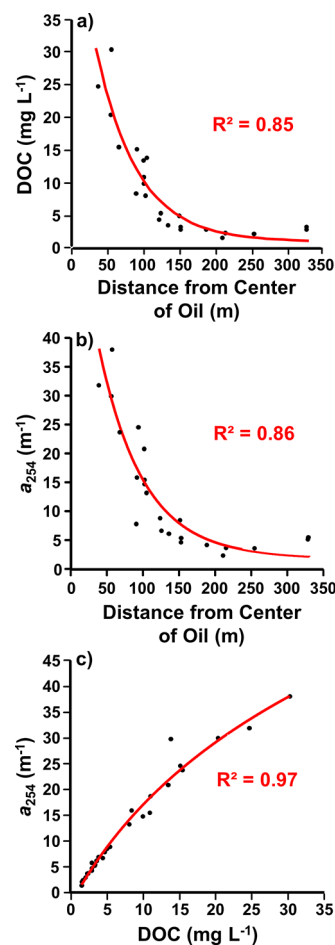


Figure 2. (a) DOC concentration and, (b) a_{254} values as a function of distance from the oil body, (c) correlation between DOC concentration and a_{254} .

pertaining to its fate and persistence in the environment even before transformations in chemical composition are determined. The model of natural attenuation at the Bemidji site predicts that the stable DOC_{HC} concentration (y_0) will be $1.14 \pm 1.55 \text{ mg L}^{-1}$. This predicted value is highly comparable to DOC concentrations measured in background wells 310B and 310E (1.66 and 1.27 mg L^{-1} respectively). Although comparable DOC concentrations suggest $\sim 100\%$ mineralization of DOC_{HC} over time and that DOC concentrations in the groundwater can return to background levels because of natural attenuation processes, section 3.2 will describe how the composition of the pool of petroleum-derived dissolved organic matter (DOM_{HC}) after natural attenuation is different from the dissolved organic matter (DOM) in the native groundwater. Moreover, eq 1 provides a relative natural attenuation rate of the DOC_{HC} of $\sim 0.11\% \text{ d}^{-1}$ ($40\% \text{ yr}^{-1}$), which is in general agreement with previous reports.⁶⁰ In addition to predicting the final DOC_{HC} concentration and the relative rate of natural attenuation, the model provides the time (distance from the source) at which the natural attenuation process stops. This information in combination with the composition and acute toxicity of the DOM_{HC} is critical for understanding the true impacts of a spill, assessing the mobilization of petroleum into the surrounding ecosystem, and assessing its potential impacts and fate. Below we highlight methodology to obtain the data required to develop these models with relatively inexpensive,

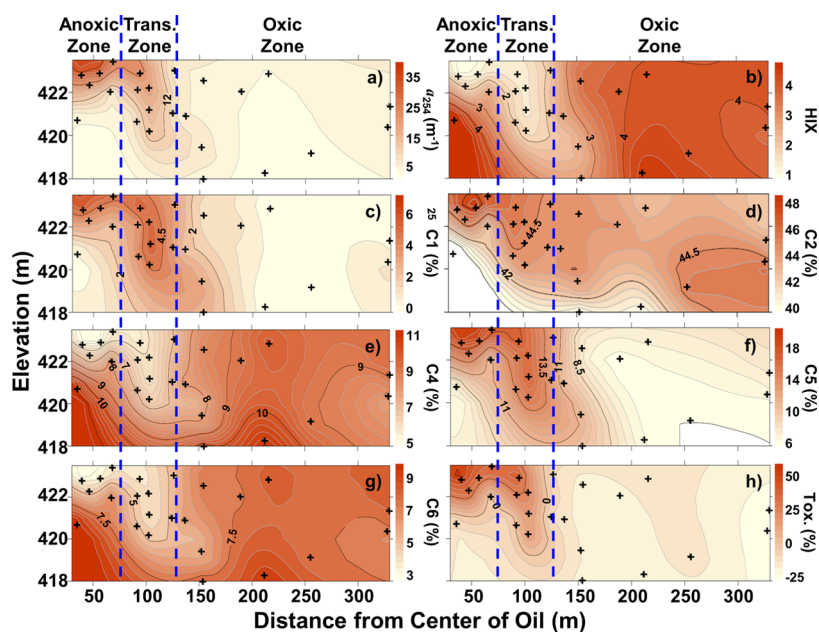


Figure 3. Contour plots showing changes in (a) a_{254} , (b) HIX, % relative contribution of PARAFAC components (c) C1, (d) C2, (e) C4, (f) C5, (g) C6, and (h) % bioluminescence inhibition (acutely toxic)/stimulation (not acutely toxic).

rapid and robust optical techniques that can provide high spatial and temporal resolution measurements to determine the composition and potential toxicity of DOM_{HC} in groundwater systems.^{62–64}

3.2. Assessing Natural Attenuation with Optical Spectroscopy. A suite of parameters and indices from optical spectroscopy measurements were examined to assess transformations in the composition of DOM_{HC} originating from the north oil pool due to natural attenuation processes (Figure 3). Absorbance at 254 nm (a_{254}), humification index (HIX) and the relative contribution of six PARAFAC components (C1–6) were determined for the DOM_{HC} sampled from each well. Three dimensional color contour plots of these values measured for the DOM_{HC} in the north oil plume are shown in Figure 3. Each well shown in Figure 3 (starting with those adjacent to the oil body) is denoted by (+) and is plotted based on the distance downgradient from the center of the north oil pool and elevation above sea level. The data for water samples that were in direct contact with oil are not included in Figure 3 as they distort the contour plots in some instances due to the overwhelming absorbance and fluorescence signal of the DOM_{HC} emitted directly from the oil body (Table S1). Each measured or modeled value discussed below provides valuable insight into strategies for rapid, cost-effective examination of natural attenuation at contaminated groundwater sites.

Previous studies have reported a strong positive correlation between CDOM absorbance at 254 nm (a_{254}) and DOC concentration.^{17,65,66} Examining a_{254} values in the wells from the north oil pool, it is apparent that the a_{254} values are highest for the CDOM_{HC} in the groundwater directly in contact (Table S1) and adjacent to the oil body (Figure 3a). Along the centerline of the plume, a_{254} values decrease as the CDOM_{HC} moves away from the source to a minimum value of 2.4 m^{-1} at a distance $\sim 211 \text{ m}$ from the oil body (Figure 3a). Similarly, Figure 2b exhibits an exponential decrease in a_{254} as observed for DOC_{HC} concentration as a function of distance from the center of the oil pool. The similarity is striking when modeling a_{254} values with the same equation (eq 1) as the DOC_{HC} data

(Figure 2). Notably, the resulting R^2 value of 0.86 for a_{254} is highly comparable to the R^2 value of 0.85 modeled from the DOC_{HC} data. Moreover, Figure 2c shows that there is a strong positive correlation ($R^2 = 0.97$) between DOC_{HC} concentration and a_{254} at the Bemidji site. The reason why the correlation is not linear is likely due to the change in composition from relatively aliphatic to aromatic DOM_{HC} because of biodegradation. This correlation indicates that optical spectroscopy can be used to examine natural attenuation of the DOC_{HC} at this oil spill site. The strong relationship between a_{254} and DOC_{HC} highlights that the same information obtained from modeling the DOC_{HC} data directly to quantify the stable DOC_{HC} pool and determine relative rates of natural attenuation, may also be determined directly from solely the a_{254} data. Indeed, the final predicted a_{254} value obtained from eq 1 of the stable CDOM_{HC} pool is $1.84 \pm 2.24 \text{ m}^{-1}$. The relationship between a_{254} and DOC_{HC} enables the conversion of the modeled a_{254} value to predict a final stable DOC_{HC} concentration of 1.59 mg L^{-1} , which is comparable to the DOC concentration measured for the groundwater in both background wells. Finally, the relative rate of natural attenuation determined from a_{254} values of $0.10\% \text{ d}^{-1}$ ($35\% \text{ yr}^{-1}$) is similar to that determined from direct DOC measurements emphasizing the validity of using the optical absorbance data to determine natural attenuation of DOC_{HC} at the site.

Apparent humification results from mineralization of aliphatic, low MW compounds and selective preservation of aromatic, high MW compounds from biodegradation.⁶⁷ Discerning relative changes in the humification index (HIX) enables the examination of this microbially driven process via optical spectroscopy.²³ The HIX values measured in the wells transecting the DOM_{HC} plume originating from the north oil pool show how biodegradation transforms this material, with low values representing newly formed DOM_{HC} that is aliphatic with low oxygen content and high values representing aromatic DOM_{HC} with high oxygen content that is selectively preserved due to biodegradation (Figure 3b). The samples collected from the wells under the oil body and nearest to the source exhibit

the lowest HIX values whereas those 328 m downgradient are the highest (Table S1). Directly beneath the center of the oil body, the HIX value is 0.6. This value increases to 1.1 approximately 56 m downgradient and then increases further to 1.6 for the DOM_{HC} in the center of the plume ~100 m downgradient. Within the next 100 m (100–200 m downgradient from the center of the oil body), the HIX values increase steeply along this distance to a value greater than 4. The sharp onset of humification is consistent with DOM_{HC} leaving the anoxic groundwater zone (75 m from the center of the oil body), moving through the transition zone extending ~125 m downgradient, to the oxic zone in the aquifer (Figure 3).^{47,68} The transition from an anaerobic to aerobic degradation process increases the mineralization rate of relatively aliphatic DOM_{HC}, reflected by the increasing HIX values downgradient from the oil body.

PARAFAC Component 1 (C1) is the most blue-shifted component in this study with excitation maxima at <250 and 280 nm and emission maximum at 306 nm. Historically, this component was described as tyrosine-like, one of two components that typically comprise the protein-like region of fluorescence.^{69,70} Component 2 (C2) is slightly red-shifted relative to C1 with excitation maxima at <250 and 285 nm and emission maximum at 375 nm. An identical component has been described in samples collected from the Amazon River Basin⁷¹ and C2 is likely composed of compounds with low MW, relatively high aromaticity ($H/C < 1$), and high O/C . Each spectrum for components 3 (C3), 4 (C4) and 6 (C6) are relatively red-shifted, corresponding with different humic/fulvic acid-like signatures. The excitation maxima at <250 and 305 nm and emission maximum at 437 nm measured for C3 is interpreted as humic-like Peak A, a region associated with relatively aromatic, high MW compounds.^{72–75} The spectrum for C4 with excitation maximum at 305 nm and emission maximum at 416 nm is similar to the microbial-derived humic Peak M, characterized as relatively aliphatic, low MW DOM.^{13,76,77} Component 6 has excitation maxima at 265 and 365 nm and emission maximum at 474 nm. This UV and visible (Peak A, C) region is ubiquitous in freshwater ecosystems and is likely a signature of highly degraded, aromatic DOM.^{13,29,72,78} The component termed C5 is slightly red-shifted from C1 with an excitation maximum at 275 nm and emission maximum at 325 nm. The common term for fluorescence in this region is tryptophan-like and collectively with C1 (tyrosine-like), comprises the region associated with protein-like DOM.^{37,79,80} These components are noteworthy because they are thought to be derived from aromatic amino acids that have been shown to represent biolabile or semibiolabile pools of DOM.^{81,82} In addition to matching tryptophan-like components in the OpenFluor database, C5 also matches components that have been associated with dissolved polynuclear aromatic hydrocarbons (PAHs).⁸³

The contour plots (Figure 3c–g) show the percent relative contributions of C1–C2 and C4–C6 as a function of distance from the center of the oil body. Component 3 is not included in the figure because it is similar to C6 in composition and behavior in the system (C3 vs C6 $R^2 = 0.91$) (Table S1; Figure 3, S2). With respect to the contour plots for the humic/fulvic acid-like components (C3, C4, and C6) each of these components exhibits its minimum value in the DOM_{HC} collected from wells beneath and adjacent to the source (Figure 3; Table S1). The value of C2, the component associated with compounds with low MW, relatively high

aromaticity ($H/C < 1$), and high O/C , ranges from 34 to 45% beneath the oil body (Table S1) and ~46% in the DOM_{HC} collected adjacent to the oil body (Figure 3d). The value for this component remains relatively constant along the DOM_{HC} plume transect, an indication that this component may represent a biorefractory component of DOM_{HC} that can be used as a tracer (Figure 3d; Figure S2). The relative contribution of C4, the humic-like signature associated with relatively low molecular weight, aliphatic compounds, is ~5% under/adjacent to the oil body and increases to ~7% at 100 m before reaching a maximum value of ~11% at 200 m from the center of the oil (Figure 3e; Figure S2). Similar to C3 and C4, the most red-shifted of the humic/fulvic acid-like components (C6) accounts for ~3% of the total contribution under/adjacent to the source and then reaches its maximum of ~10% at a distance of 200 m from the center of the oil body (Figure 3g; Figure S2). Although relative contributions of the red-shifted humic/fulvic-like components C3 (~33%), C4 (~11%), and C6 (~10%) increase as a function of distance from the oil body, they are still significantly different from the average values of these three components measured for the DOM in the background wells of ~23%, 28%, and 25%, respectively (Table S1). This result indicates that the DOM_{HC} retains a unique optical signature during biodegradation.

PARAFAC component C1, characterized as the tyrosine-like fluorophore, exhibits a maximum relative contribution in the DOM_{HC} collected from the wells directly beneath the oil body (Table S1). Here, the relative contribution of C1 accounts for up to ~16% (Table S1) and ~7% (Figure 3c) beneath and adjacent to the oil body respectively, of the total contribution of the PARAFAC components. The contribution of C1 decreases to ~2% at a distance of ~150 m from the center of the oil body and is almost completely removed at a distance of 200 m (Figure 3c; Figure S2; Table S1). Component C1 is not present at all in the background wells (Table S1), an indication that the DOM with this signature is petroleum-derived at this site. Although the chemical characteristics of C1 are similar to tyrosine, the fluorescence comprising C1 at the spill site is more likely to be (alkyl-substituted) benzene derivatives.³⁹ These classes of compounds are also biolabile or semibiolabile as reported in past studies^{81,82} and biological degradation of these compounds would match the observed trends for C1 shown in Figures 3c and Figure S2.

Beneath the oil body, the relative contribution of C5 is at its maximum measured value of 49.4% (Table S1) with a contribution ~19% directly adjacent to the body (Figure 3f). Within a distance of 100 m downgradient, the relative contribution of C5 decreases to ~13% before reaching a minimum value of ~6% at a distance of 250 m downgradient of the oil body (Figure 3f; Figure S2). Unlike C1, C5 is present in the background wells and those farthest away from the oil body, an indication that some of the relative contribution of C5 is from naturally sourced tryptophan-like DOM fluorescence. There is, however, a significant increase in C5 in the DOM_{HC} collected under and adjacent to the oil body relative to that in the background wells (Table S1) indicating that DOM_{HC} contributes to the fluorescence in this region. The red shift in excitation and emission maxima of C5 relative to C1 is an indication that these DOM_{HC} compounds may be similar to (alkyl-substituted) naphthalene derivatives.³⁹ Similar to C1 and previous reports for protein-like fluorescence,⁸⁰ the decrease in the relative contribution of C5 to near background levels shows

that the DOM_{HC} attributed to C5 is composed of biolabile or semibiolabile compounds.

A principal component analysis (PCA) plot that includes values for C1–C6, HIX, and a_{254} for all the wells including background sites listed in Table S1 provides a composite visualization of natural attenuation of DOM_{HC} originating from the north oil body at the Bemidji research site (Figure 1). The most important feature of this plot is that all of the loadings are from optical measurements. The largest percentage of the variance is in PCA 1 (61.3%) and the main drivers of PCA 1 are $CDOM_{HC}$ (e.g., Figure 2b), blue-shifted (C1 and C5) and red-shifted (C4 and C6) PARAFAC components. The darkest shaded markers depict wells directly under the oil body, the lightest are those farthest downgradient from the center of the oil body, the red markers represent the background wells.

Blue-shifted fluorescence signatures (C1 and C5) dominate the DOM_{HC} produced directly beneath and adjacent to the oil body. Moreover, absorbance at 254 nm indicates that the highest DOC_{HC} concentrations are directly under the oil body and that natural attenuation of the DOM_{HC} occurs as it migrates downgradient from the oil body with the groundwater as evidenced by the clear compositional trend toward relatively aromatic, oxygenated red-shifted fluorescence (C4 and C6) similar to the DOM measured in the background wells (Figure 1).^{8,84–88} It is noteworthy that wells can be identified that are outside or on the edge of the main contamination plume (S33C and S31C) in the PCA plot (Figure 1). Although the water from wells S33C and S31C have optical signatures consistent with DOM_{HC} (Table S1), the composition of DOM_{HC} in these wells suggest that they are on the outer edge of the plume where attenuation rates are higher due the presence of oxygen. Moreover, the PCA plot shows that although the degradation of DOM_{HC} is prevalent from natural attenuation and the general trend is toward the composition of the DOM in the background wells, it not completely attenuated when examining optical parameters. Dissolved compounds that partition into the water beneath the oil such as those that result in the increase in the relative contribution of C2 (>25%) persist across the entire plume transect (Figure S2; Table S1). This result suggests that the Unnamed Lake located 325 m downgradient of the north pool oil body is receiving a supply of DOM_{HC} that retains compositional similarities of the petroleum source from which it was produced.

The plots depicted in Figure S2 show how the relative contribution of each PARAFAC component changes as a function of distance from the center of the oil body and highlight the compositional “transformations” in the collective DOM_{HC} pool because of biodegradation. Although the apparent transformation in the composition of the DOM_{HC} pool is a result of selective preservation, these data provide evidence of a biodegradation continuum (Figures 1; 2 and S2). Utilization of optical spectroscopy to define and study this continuum provides a method to monitor biodegradation of DOM_{HC} , especially in contaminated groundwater systems. These concepts may also be applied for examining other emerging contaminants in the environment.⁸⁹

3.3. Acute Toxicity. A subset of the wells sampled along the transect were screened for acute toxicity. Examination of this toxicity data as a function of distance from the center of the oil body (Figure 3h) shows that the wells adjacent to the oil body had highest toxicity. The maximum toxicity (51% bioluminescence inhibition) was measured at well S33E (34 m from the center of the oil body; Table S1). The

bioluminescence inhibition rapidly decreased to zero (i.e., no acute toxicity) from 34 to 100 m from the center of the oil body. Bioluminescence values less than zero are considered to be a result of stimulation of bacterial metabolic activity (Table S1). Stimulation (relative to control) may have been a result of substantial reduction or removal of chemicals responsible for acute toxicity. Such reductions could have led to hormetic effects (positive effects at very low chemical concentrations have been described⁹⁰), and/or once acute toxicity was removed, stimulatory effects of other less toxic chemicals/nutrients could have been detected. Alternatively, stimulatory effects may have been caused by chemical-induced uncoupling of a proton gradient and associated increases in enzyme system associated with light production.⁹¹

The addition of toxicity as a loading into a PCA plot with optical measurements shows that toxicity clusters with C1, C2, and a_{254} (Figure S3). Relationships between all of the optical parameters and Microtox results were examined by linear regression analysis to determine if any of them can be used for identifying potentially toxic DOM_{HC} in the field. Both a_{254} and C5 were positively correlated with acute toxicity (indicated by bioluminescence inhibition), whereas HIX, C3, C4, and C6 are negatively correlated with acute toxicity ($R^2 > 0.5$). Conversely, C1 and C2 exhibit no correlation with acute toxicity ($R^2 < 0.3$). C5 was found to exhibit a positive relationship with toxicity values >0 ($R^2 = 0.60$) and a discrete value (14% relative contribution) that separated inhibition and stimulation in the Microtox results (Figure 4). These data were modeled with a 4-

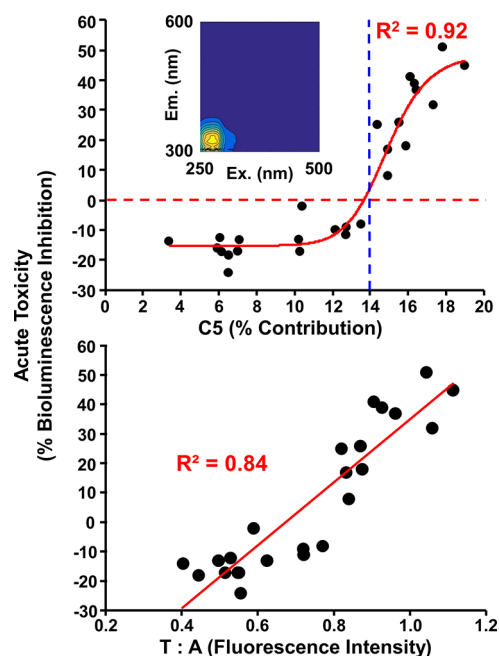


Figure 4. Relative contribution of PARAFAC component 5 (C5) vs percent bioluminescence inhibition (top). Ratio of raw fluorescence of Peaks T and A vs percent bioluminescence inhibition (bottom).

parameter logistic regression equation to further investigate the relationship between C5 and acute toxicity (Figure 4). This model provides a $R^2 = 0.92$ and shows a division between inhibition and stimulation results occurs at a relative contribution value of 14% for C5 (Figure 4). The correlation between C5 and Microtox values shows that optical spectroscopy, combined with rapid acute toxicity assessment (i.e.,

Microtox) has the potential as a screening tool for identification of potentially toxic DOM_{HC} at contaminated sites.

Microtox measurements were not completed on any of the water samples collected directly under the oil body (604A, 306, 421B, and 534A) and two wells downgradient from the oil body (9316C and 1217C) (Table S1). However, the four wells under the oil body each exhibit relative contributions of C5 > 14% and the 2 wells >150 m downgradient from the oil body are <14% C5. The relationship between the relative contribution of C5 and the Microtox analyses leads us to predict that the water collected from directly under the oil body is acutely toxic, whereas the wells downgradient are not acutely toxic. These results from the Bemidji north oil pool suggests that optical parameters such as tracing fluorophores may offer a robust tool for screening potentially toxic waters impacted by oil spills.

Although PARAFAC is a useful tool for assessing changes in the composition of the DOM_{HC} pool and determining relationships between composition and acute toxicity, it is relatively complicated to implement. However, the information obtained by PARAFAC analysis informs us that C5, the component that shows a strong positive correlation with acute toxicity, is similar to “tryptophan-like” fluorescence. Tryptophan-like fluorescence, commonly referred to as “Peak T”, has Ex./Em. maxima at 290/350 nm. Rapid screening methods can be implemented by using the ratio of raw fluorescence of Peak T and one of the ubiquitous humic/fulvic-like fluorescence signatures such as “Peak A” (Ex./Em. 250/450 nm) (Figure 4). Figure 4 shows a positive correlation between the ratio of Peaks A:C and acute toxicity ($R^2 = 0.84$) and portable spectrophotometers are becoming increasingly available that can measure these fluorescence signatures highlighting the potential for future studies to assess real-time toxicity for oil spills.^{62,92,93}

■ ASSOCIATED CONTENT

Supporting Information

The Supporting Information is available free of charge on the ACS Publications website at DOI: 10.1021/acs.est.8b00016.

Comparison of PARAFAC components, changes in PARAFAC components, PCA plot of optical properties and acute toxicity, well information, DOC, optical values, acute toxicity (PDF)

■ AUTHOR INFORMATION

Corresponding Author

*Tel.: +1-504-280-4438. E-mail address: dcpodgor@uno.edu (D. C. Podgorski).

ORCID

David C. Podgorski: 0000-0002-1070-5923

Isabelle M. Cozzarelli: 0000-0002-5123-1007

Notes

The authors declare no competing financial interest.

■ ACKNOWLEDGMENTS

NVDOC data generated during this study are available at <https://doi.org/10.5066/F7CN733T>.⁹⁴ This work was supported by the 2017 Enbridge Ecofootprint Grant awarded by the Minnesota Association of Resource Conservation and Development (Project #1703033), U.S. Geological Survey Toxic Substances Hydrology Program, and the National High Magnetic Field Laboratory (NSF DMR-1157490). D.C.P. and

R.G.M.S. were partially supported by NSF OCE-1333157 and OCE-1464396. The authors thank Jared Trost, Ean Warren, Andrew Berg, Jeanne Jaeschke, and the rest of the Bemidji research team for their assistance. The authors also thank the three anonymous reviewers and Jeffery Steevens from the U.S. Geological Survey Fish and Invertebrate Toxicology Branch for their contributions.

■ REFERENCES

- (1) Aeppli, C.; Carmichael, C. A.; Nelson, R. K.; Lemkau, K. L.; Graham, W. M.; Redmond, M. C.; Valentine, D. L.; Reddy, C. M. Oil Weathering after the Deepwater Horizon Disaster Led to the Formation of Oxygenated Residues. *Environ. Sci. Technol.* **2012**, *46* (16), 8799–8807.
- (2) von Netzer, F.; Piloni, G.; Kleindienst, S.; Kruger, M.; Knittel, K.; Grundger, F.; Lueders, T. Enhanced Gene Detection Assays for Fumarate-Adding Enzymes Allow Uncovering of Anaerobic Hydrocarbon Degraders in Terrestrial and Marine Systems. *Appl. Environ. Microbiol.* **2013**, *79* (2), 543–552.
- (3) Hazen, T. C.; Prince, R. C.; Mahmoudi, N. Marine Oil Biodegradation. *Environ. Sci. Technol.* **2016**, *50* (5), 2121–2129.
- (4) Townsend, G. T.; Prince, R. C.; Suflija, J. M. Anaerobic oxidation of crude oil hydrocarbons by the resident microorganisms of a contaminated anoxic aquifer. *Environ. Sci. Technol.* **2003**, *37* (22), 5213–5218.
- (5) Anderson, R. T.; Rooney-Varga, J. N.; Gaw, C. V.; Lovley, D. R. Anaerobic benzene oxidation in the Fe(III) reduction zone of petroleum contaminated aquifers. *Environ. Sci. Technol.* **1998**, *32* (9), 1222–1229.
- (6) Amos, R. T.; Bekins, B. A.; Cozzarelli, I. M.; Voytek, M. A.; Kirshtein, J. D.; Jones, E. J. P.; Blowes, D. W. Evidence for iron-mediated anaerobic methane oxidation in a crude oil-contaminated aquifer. *Geobiology* **2012**, *10* (6), 506–517.
- (7) Essaid, H. I.; Bekins, B. A.; Herkelrath, W. N.; Delin, G. N. Crude Oil at the Bemidji Site: 25 Years of Monitoring, Modeling, and Understanding. *Groundwater* **2011**, *49* (5), 706–726.
- (8) Ray, P. Z.; Chen, H.; Podgorski, D. C.; McKenna, A. M.; Tarr, M. A. Sunlight creates oxygenated species in water-soluble fractions of Deepwater horizon oil. *J. Hazard. Mater.* **2014**, *280*, 636–643.
- (9) Bekins, B. A.; Cozzarelli, I. M.; Erickson, M. L.; Steenson, R. A.; Thorn, K. A. Crude Oil Metabolites in Groundwater at Two Spill Sites. *Groundwater* **2016**, *54* (5), 681–691.
- (10) Lundstedt, S.; White, P. A.; Lemieux, C. L.; Lynes, K. D.; Lambert, L. B.; Oberg, L.; Haglund, P.; Tysklind, M. Sources, fate, and toxic hazards of oxygenated polycyclic aromatic hydrocarbons (PAHs) at PAH-contaminated sites. *Ambio* **2007**, *36* (6), 475–485.
- (11) Wincent, E.; Jonsson, M. E.; Bottai, M.; Lundstedt, S.; Dreij, K. Aryl Hydrocarbon Receptor Activation and Developmental Toxicity in Zebrafish in Response to Soil Extracts Containing Unsubstituted and Oxygenated PAHs. *Environ. Sci. Technol.* **2015**, *49* (6), 3869–3877.
- (12) Carney, M. W.; Erwin, K.; Hardman, R.; Yuen, B.; Volz, D. C.; Hinton, D. E.; Kullman, S. W. Differential developmental toxicity of naphthoic acid isomers in medaka (*Oryzias latipes*) embryos. *Mar. Pollut. Bull.* **2008**, *57* (6–12), 255–266.
- (13) Coble, P. G.; Del Castillo, C. E.; Avril, B. Distribution and optical properties of CDOM in the Arabian Sea during the 1995 Southwest Monsoon. *Deep Sea Res., Part II* **1998**, *45* (10–11), 2195–2223.
- (14) Del Vecchio, R.; Blough, N. V. Spatial and seasonal distribution of chromophoric dissolved organic matter and dissolved organic carbon in the Middle Atlantic Bight. *Mar. Chem.* **2004**, *89* (1–4), 169–187.
- (15) Weiss, J. V.; Cozzarelli, I. M.; Lowit, M. B.; Voytek, M. A. Biodegradable Carbon as a Potential Control on Microbial Community Structure and Function in an Aquifer Contaminated with Landfill Leachate; Geological Society of America, 2005; Vol. 37, p 474.

- (16) Osburn, C. L.; Wigdahl, C. R.; Fritz, S. C.; Saros, J. E. Dissolved organic matter composition and photoreactivity in prairie lakes of the U.S. Great Plains. *Limnol. Oceanogr.* **2011**, *56* (6), 2371–2390.
- (17) Spencer, R. G. M.; Butler, K. D.; Aiken, G. R. Dissolved organic carbon and chromophoric dissolved organic matter properties of rivers in the USA. *J. Geophys Res-Biogeosci.* **2012**, *117*, 1–14.
- (18) Mann, P. J.; Spencer, R. G. M.; Hernes, P. J.; Six, J.; Aiken, G. R.; Tank, S. E.; McClelland, J. W.; Butler, K. D.; Dyda, R. Y.; Holmes, R. M. Pan-Arctic Trends in Terrestrial Dissolved Organic Matter from Optical Measurements. *Front Earth Sci.* **2016**, *4*, 1–18.
- (19) Hansen, A. M.; Kraus, T. E. C.; Pellerin, B. A.; Fleck, J. A.; Downing, B. D.; Bergamaschi, B. A. Optical properties of dissolved organic matter (DOM): Effects of biological and photolytic degradation. *Limnol. Oceanogr.* **2016**, *61* (3), 1015–1032.
- (20) Moran, M. A.; Sheldon, W. M.; Zepp, R. G. Carbon loss and optical property changes during long-term photochemical and biological degradation of estuarine dissolved organic matter. *Limnol. Oceanogr.* **2000**, *45* (6), 1254–1264.
- (21) Chin, Y. P.; Aiken, G.; O'Loughlin, E. Molecular-Weight, Polydispersity, and Spectroscopic Properties of Aquatic Humic Substances. *Environ. Sci. Technol.* **1994**, *28* (11), 1853–1858.
- (22) McKnight, D. M.; Boyer, E. W.; Westerhoff, P. K.; Doran, P. T.; Kulbe, T.; Andersen, D. T. Spectrofluorometric characterization of dissolved organic matter for indication of precursor organic material and aromaticity. *Limnol. Oceanogr.* **2001**, *46* (1), 38–48.
- (23) Ohno, T. Fluorescence inner-filtering correction for determining the humification index of dissolved organic matter. *Environ. Sci. Technol.* **2002**, *36* (4), 742–746.
- (24) Weishaar, J. L.; Aiken, G. R.; Bergamaschi, B. A.; Fram, M. S.; Fujii, R.; Mopper, K. Evaluation of specific ultraviolet absorbance as an indicator of the chemical composition and reactivity of dissolved organic carbon. *Environ. Sci. Technol.* **2003**, *37* (20), 4702–4708.
- (25) Helms, J. R.; Stubbins, A.; Ritchie, J. D.; Minor, E. C.; Kieber, D. J.; Mopper, K. Absorption spectral slopes and slope ratios as indicators of molecular weight, source, and photobleaching of chromophoric dissolved organic matter. *Limnol. Oceanogr.* **2008**, *53* (3), 955–969.
- (26) Spencer, R. G. M.; Aiken, G. R.; Butler, K. D.; Dornblaser, M. M.; Striegl, R. G.; Hernes, P. J. Utilizing chromophoric dissolved organic matter measurements to derive export and reactivity of dissolved organic carbon exported to the Arctic Ocean: A case study of the Yukon River, Alaska. *Geophys. Res. Lett.* **2009**, *36*, 1–6.
- (27) Boyle, E. S.; Guerriero, N.; Thiallet, A.; Del Vecchio, R.; Blough, N. V. Optical Properties of Humic Substances and CDOM: Relation to Structure. *Environ. Sci. Technol.* **2009**, *43* (7), 2262–2268.
- (28) Andrew, A. A.; Del Vecchio, R.; Subramaniam, A.; Blough, N. V. Chromophoric dissolved organic matter (CDOM) in the Equatorial Atlantic Ocean: Optical properties and their relation to CDOM structure and source. *Mar. Chem.* **2013**, *148*, 33–43.
- (29) Stedmon, C. A.; Markager, S.; Bro, R. Tracing dissolved organic matter in aquatic environments using a new approach to fluorescence spectroscopy. *Mar. Chem.* **2003**, *82* (3–4), 239–254.
- (30) Cory, R. M.; McKnight, D. M. Fluorescence spectroscopy reveals ubiquitous presence of oxidized and reduced quinones in dissolved organic matter. *Environ. Sci. Technol.* **2005**, *39* (21), 8142–8149.
- (31) Jaffe, R.; McKnight, D.; Maie, N.; Cory, R.; McDowell, W. H.; Campbell, J. L. Spatial and temporal variations in DOM composition in ecosystems: The importance of long-term monitoring of optical properties. *J. Geophys Res-Biogeosci.* **2008**, *113* (G4), 1–15.
- (32) Murphy, K. R.; Stedmon, C. A.; Waite, T. D.; Ruiz, G. M. Distinguishing between terrestrial and autochthonous organic matter sources in marine environments using fluorescence spectroscopy. *Mar. Chem.* **2008**, *108* (1–2), 40–58.
- (33) Cao, F.; Medeiros, P. M.; Miller, W. L. Optical characterization of dissolved organic matter in the Amazon River plume and the Adjacent Ocean: Examining the relative role of mixing, photochemistry, and microbial alterations. *Mar. Chem.* **2016**, *186*, 178–188.
- (34) Kim, M.; Yim, U. H.; Hong, S. H.; Jung, J. H.; Choi, H. W.; An, J.; Won, J.; Shim, W. J. Hebei Spirit oil spill monitored on site by fluorometric detection of residual oil in coastal waters off Taean, Korea. *Mar. Pollut. Bull.* **2010**, *60* (3), 383–389.
- (35) Zhou, Z. Z.; Liu, Z. F.; Guo, L. D. Chemical evolution of Macondo crude oil during laboratory degradation as characterized by fluorescence EEMs and hydrocarbon composition. *Mar. Pollut. Bull.* **2013**, *66* (1–2), 164–175.
- (36) Zhou, Z. Z.; Guo, L. D.; Shiller, A. M.; Lohrenz, S. E.; Asper, V. L.; Osburn, C. L. Characterization of oil components from the Deepwater Horizon oil spill in the Gulf of Mexico using fluorescence EEM and PARAFAC techniques. *Mar. Chem.* **2013**, *148*, 10–21.
- (37) Bianchi, T. S.; Osburn, C.; Shields, M. R.; Yvon-Lewis, S.; Young, J.; Guo, L. D.; Zhou, Z. Z. Deepwater Horizon Oil in Gulf of Mexico Waters after 2 Years: Transformation into the Dissolved Organic Matter Pool. *Environ. Sci. Technol.* **2014**, *48* (16), 9288–9297.
- (38) Dvorski, S. E. M.; Gonsior, M.; Hertkorn, N.; Uhl, J.; Muller, H.; Griebler, C.; Schmitt-Kopplin, P. Geochemistry of Dissolved Organic Matter in a Spatially Highly Resolved Groundwater Petroleum Hydrocarbon Plume Cross-Section. *Environ. Sci. Technol.* **2016**, *50* (11), 5536–5546.
- (39) Mendoza, W. G.; Riemer, D. D.; Zika, R. G. Application of fluorescence and PARAFAC to assess vertical distribution of subsurface hydrocarbons and dispersant during the Deepwater Horizon oil spill. *Environ. Sci.-Proc. Imp.* **2013**, *15* (5), 1017–1030.
- (40) Keizer, P. D.; Gordon, D. C., Jr. Detection of Trace Amounts of Oil in Sea Water by Fluorescence Spectroscopy. *J. Fish. Res. Board Can.* **1973**, *30* (8), 1039–1046.
- (41) Bugden, J. B. C.; Yeung, C. W.; Kepkay, P. E.; Lee, K. Application of ultraviolet fluorometry and excitation-emission matrix spectroscopy (EEMS) to fingerprint oil and chemically dispersed oil in seawater. *Mar. Pollut. Bull.* **2008**, *56* (4), 677–685.
- (42) Bugden, J. B.; Yeung, C. W.; Kepkay, P. E.; Lee, K. Application of ultraviolet fluorometry and excitation-emission matrix spectroscopy (EEMS) to fingerprint oil and chemically dispersed oil in seawater. *Mar. Pollut. Bull.* **2008**, *56* (4), 677–85.
- (43) Brown, C. E.; Fingas, M. F. Review of the development of laser fluorosensors for oil spill application. *Mar. Pollut. Bull.* **2003**, *47* (9–12), 477–84.
- (44) Fingas, M.; Brown, C. Review of oil spill remote sensing. *Mar. Pollut. Bull.* **2014**, *83* (1), 9–23.
- (45) Conmy, R. N.; Coble, P. G.; Farr, J.; Wood, A. M.; Lee, K.; Pegaw, W. S.; Walsh, I. D.; Koch, C. R.; Abercrombie, M. I.; Miles, M. S.; Lewis, M. R.; Ryan, S. A.; Robinson, B. J.; King, T. L.; Kelble, C. R.; Lacoste, J. Submersible optical sensors exposed to chemically dispersed crude oil: wave tank simulations for improved oil spill monitoring. *Environ. Sci. Technol.* **2014**, *48* (3), 1803–10.
- (46) Eganhouse, R. P.; Baedecker, M. J.; Cozzarelli, I. M.; Aiken, G. R.; Thorn, K. A.; Dorsey, T. F. Crude-Oil in a Shallow Sand and Gravel Aquifer 0.2. Organic Geochemistry. *Appl. Geochem.* **1993**, *8* (6), 551–567.
- (47) Baedecker, M. J.; Cozzarelli, I. M.; Eganhouse, R. P.; Siegel, D. I.; Bennett, P. C. Crude-Oil in a Shallow Sand and Gravel Aquifer 0.3. Biogeochemical Reactions and Mass-Balance Modeling in Anoxic Groundwater. *Appl. Geochem.* **1993**, *8* (6), 569–586.
- (48) Fahrenfeld, N.; Cozzarelli, I. M.; Bailey, Z.; Pruden, A. Insights into Biodegradation Through Depth-Resolved Microbial Community Functional and Structural Profiling of a Crude-Oil Contaminant Plume. *Microb. Ecol.* **2014**, *68* (3), 453–462.
- (49) Cozzarelli, I. M.; Schreiber, M. E.; Erickson, M. L.; Ziegler, B. A. Arsenic Cycling in Hydrocarbon Plumes: Secondary Effects of Natural Attenuation. *Groundwater* **2016**, *54* (1), 35–45.
- (50) Spencer, R. G. M.; Bolton, L.; Baker, A. Freeze/thaw and pH effects on freshwater dissolved organic matter fluorescence and absorbance properties from a number of UK locations. *Water Res.* **2007**, *41* (13), 2941–2950.
- (51) Tfaily, M. M.; Podgorski, D. C.; Corbett, J. E.; Chanton, J. P.; Cooper, W. T. Influence of acidification on the optical properties and molecular composition of dissolved organic matter. *Anal. Chim. Acta* **2011**, *706* (2), 261–267.

- (52) Yan, M. Q.; Fu, Q. W.; Li, D. C.; Gao, G. F.; Wang, D. S. Study of the pH influence on the optical properties of dissolved organic matter using fluorescence excitation-emission matrix and parallel factor analysis. *J. Lumin.* **2013**, *142*, 103–109.
- (53) Kowalczyk, P.; Cooper, W. J.; Whitehead, R. F.; Durako, M. J.; Sheldon, W. Characterization of CDOM in an organic-rich river and surrounding coastal ocean in the South Atlantic Bight. *Aquat. Sci.* **2003**, *65* (4), 384–401.
- (54) Murphy, K. R.; Stedmon, C. A.; Graeber, D.; Bro, R. Fluorescence spectroscopy and multi-way techniques. *PARAFAC. Anal. Methods* **2013**, *5* (23), 6557–6566.
- (55) Harshman, R. How can I know if it's real? A catalog of diagnostics for use with three-mode factor analysis and multidimensional scaling. In *Research methods for multimode data analysis*; Law, H. G., Snyder, C. W., Hattie, J. A., McDonald, R. P., Eds.; Praeger Publishers Inc., 1984; pp 566–591.
- (56) Stedmon, C. A.; Bro, R. Characterizing dissolved organic matter fluorescence with parallel factor analysis: a tutorial. *Limnol. Oceanogr.: Methods* **2008**, *6*, 572–579.
- (57) Murphy, K. R.; Stedmon, C. A.; Wenig, P.; Bro, R. OpenFluor—an online spectral library of auto-fluorescence by organic compounds in the environment. *Anal. Methods* **2014**, *6*, 658–661.
- (58) Kaiser, K. L. E. Correlations of *Vibrio fischeri* bacteria test data with bioassay data for other organisms. *Environ. Health Perspect.* **1998**, *106*, 583–591.
- (59) Dewhurst, R. E.; Wheeler, J. R.; Chummun, K. S.; Mather, J. D.; Callaghan, A.; Crane, M. The comparison of rapid bioassays for the assessment of urban groundwater quality. *Chemosphere* **2002**, *47* (5), 547–554.
- (60) Ng, G. H. C.; Bekins, B. A.; Cozzarelli, I. M.; Baedecker, M. J.; Bennett, P. C.; Amos, R. T.; Herkelrath, W. N. Reactive transport modeling of geochemical controls on secondary water quality impacts at a crude oil spill site near Bemidji, MN. *Water Resour. Res.* **2015**, *51* (6), 4156–4183.
- (61) Essaid, H. I.; Cozzarelli, I. M.; Eganhouse, R. P.; Herkelrath, W. N.; Bekins, B. A.; Delin, G. N. Inverse modeling of BTEX dissolution and biodegradation at the Bemidji, MN crude-oil spill site. *J. Contam. Hydrol.* **2003**, *67* (1–4), 269–299.
- (62) Spencer, R. G. M.; Pellerin, B. A.; Bergamaschi, B. A.; Downing, B. D.; Kraus, T. E. C.; Smart, D. R.; Dahlgren, R. A.; Hernes, P. J. Diurnal variability in riverine dissolved organic matter composition determined by in situ optical measurement in the San Joaquin River (California, USA). *Hydrol. Processes* **2007**, *21* (23), 3181–3189.
- (63) Pellerin, B. A.; Saraceno, J. F.; Shanley, J. B.; Sebestyen, S. D.; Aiken, G. R.; Wollheim, W. M.; Bergamaschi, B. A. Taking the pulse of snowmelt: in situ sensors reveal seasonal, event and diurnal patterns of nitrate and dissolved organic matter variability in an upland forest stream. *Biogeochemistry* **2012**, *108* (1–3), 183–198.
- (64) Ruhala, S. S.; Zarnetske, J. P. Using in-situ optical sensors to study dissolved organic carbon dynamics of streams and watersheds: A review. *Sci. Total Environ.* **2017**, *575*, 713–723.
- (65) Del Vecchio, R.; Blough, N. V. On the origin of the optical properties of humic substances. *Environ. Sci. Technol.* **2004**, *38* (14), 3885–3891.
- (66) Mannino, A.; Russ, M. E.; Hooker, S. B. Algorithm development and validation for satellite-derived distributions of DOC and CDOM in the US Middle Atlantic Bight. *J. Geophys. Res.* **2008**, *113* (C7), 1–19.
- (67) Zonneveld, K. A. F.; Versteegh, G. J. M.; Kasten, S.; Eglinton, T. I.; Emeis, K. C.; Huguet, C.; Koch, B. P.; de Lange, G. J.; de Leeuw, J. W.; Middelburg, J. J.; Mollenhauer, G.; Prahl, F. G.; Rethemeyer, J.; Wakeham, S. G. Selective preservation of organic matter in marine environments; processes and impact on the sedimentary record. *Biogeosciences* **2010**, *7* (2), 483–511.
- (68) Bennett, P. C.; Siegel, D. E.; Baedecker, M. J.; Hult, M. F. Crude-Oil in a Shallow Sand and Gravel Aquifer 0.1. Hydrogeology and Inorganic Geochemistry. *Appl. Geochem.* **1993**, *8* (6), 529–549.
- (69) Yamashita, Y.; Kloepfel, B. D.; Knoepf, J.; Zausen, G. L.; Jaffe, R. Effects of Watershed History on Dissolved Organic Matter Characteristics in Headwater Streams. *Ecosystems* **2011**, *14* (7), 1110–1122.
- (70) Yamashita, Y.; Boyer, J. N.; Jaffe, R. Evaluating the distribution of terrestrial dissolved organic matter in a complex coastal ecosystem using fluorescence spectroscopy. *Cont. Shelf Res.* **2013**, *66*, 136–144.
- (71) Gonsior, M.; Valle, J.; Schmitt-Kopplin, P.; Hertkorn, N.; Bastviken, D.; Luek, J.; Harir, M.; Bastos, W.; Enrich-Prast, A. Chemodiversity of dissolved organic matter in the Amazon Basin. *Biogeosciences* **2016**, *13* (14), 4279–4290.
- (72) Coble, P. G.; Green, S. A.; Blough, N. V.; Gagosian, R. B. Characterization of Dissolved Organic-Matter in the Black-Sea by Fluorescence Spectroscopy. *Nature* **1990**, *348* (6300), 432–435.
- (73) Sondergaard, M.; Stedmon, C. A.; Borch, N. H. Fate of terrigenous dissolved organic matter (DOM) in estuaries: Aggregation and bioavailability. *Ophelia* **2003**, *57* (3), 161–176.
- (74) Kothawala, D. N.; von Wachenfeldt, E.; Koehler, B.; Tranvik, L. J. Selective loss and preservation of lake water dissolved organic matter fluorescence during long-term dark incubations. *Sci. Total Environ.* **2012**, *433*, 238–246.
- (75) Osburn, C.; Boyd, T. J.; Montgomery, M. T.; Bianchi, T. S.; Coffin, R. B.; Paerl, H. W. Optical Proxies for Terrestrial Dissolved Organic Matter in Estuaries and Coastal Waters. *Front. Mar. Sci.* **2016**, *2* (127), 1–15.
- (76) Lambert, T.; Bouillon, S.; Darchambeau, F.; Massicotte, P.; Borges, A. V. Shift in the chemical composition of dissolved organic matter in the Congo River network. *Biogeosciences* **2016**, *13* (18), 5405–5420.
- (77) Cawley, K. M.; Butler, K. D.; Aiken, G. R.; Larsen, L. G.; Huntington, T. G.; McKnight, D. M. Identifying fluorescent pulp mill effluent in the Gulf of Maine and its watershed. *Mar. Pollut. Bull.* **2012**, *64* (8), 1678–1687.
- (78) Williams, C. J.; Yamashita, Y.; Wilson, H. F.; Jaffe, R.; Xenopoulos, M. A. Unraveling the role of land use and microbial activity in shaping dissolved organic matter characteristics in stream ecosystems. *Limnol. Oceanogr.* **2010**, *55* (3), 1159–1171.
- (79) Baker, A. Fluorescence excitation-emission matrix characterization of some sewage-impacted rivers. *Environ. Sci. Technol.* **2001**, *35* (5), 948–953.
- (80) Fellman, J. B.; Hood, E.; Spencer, R. G. M. Fluorescence spectroscopy opens new windows into dissolved organic matter dynamics in freshwater ecosystems: A review. *Limnol. Oceanogr.* **2010**, *55* (6), 2452–2462.
- (81) Yamashita, Y.; Tanoue, E. Distribution and alteration of amino acids in bulk DOM along a transect from bay to oceanic waters. *Mar. Chem.* **2003**, *82* (3–4), 145–160.
- (82) Davis, J.; Benner, R. Quantitative estimates of labile and semi-labile dissolved organic carbon in the western Arctic Ocean: A molecular approach. *Limnol. Oceanogr.* **2007**, *52* (6), 2434–2444.
- (83) Murphy, K. R.; Ruiz, G. M.; Dunsmuir, W. T. M.; Waite, T. D. Optimized parameters for fluorescence-based verification of ballast water exchange by ships. *Environ. Sci. Technol.* **2006**, *40* (7), 2357–2362.
- (84) Kellerman, A. M.; Guillemette, F.; Podgorski, D. C.; Aiken, G. R.; Butler, K. D.; Spencer, R. G. M. Unifying Concepts Linking Dissolved Organic Matter Composition to Persistence in Aquatic Ecosystems. *Environ. Sci. Technol.* **2018**, *52* (5), 2538–2548.
- (85) Kellerman, A. M.; Kothawala, D. N.; Dittmar, T.; Tranvik, L. J. Persistence of dissolved organic matter in lakes related to its molecular characteristics. *Nat. Geosci.* **2015**, *8* (6), 454–U52.
- (86) Harriman, B. H.; Zito, P.; Podgorski, D. C.; Tarr, M. A.; Suflita, J. M. Impact of Photooxidation and Biodegradation on the Fate of Oil Spilled During the Deepwater Horizon Incident: Advanced Stages of Weathering. *Environ. Sci. Technol.* **2017**, *51* (13), 7412–7421.
- (87) Thorn, K. A.; Aiken, G. R. Biodegradation of crude oil into nonvolatile organic acids in a contaminated aquifer near Bemidji, Minnesota. *Org. Geochem.* **1998**, *29* (4), 909–931.
- (88) Islam, A.; Ahmed, A.; Hur, M.; Thorn, K. A.; Kim, S. Molecular-level evidence provided by ultrahigh resolution mass spectrometry for

oil-derived DOC in groundwater at Bemidji, Minnesota. *J. Hazard. Mater.* **2016**, *320*, 123–132.

(89) Baker, A. Fluorescence excitation - Emission matrix characterization of river waters impacted by a tissue mill effluent. *Environ. Sci. Technol.* **2002**, *36* (7), 1377–1382.

(90) Deng, Z. Q.; Lin, Z. F.; Zou, X. M.; Yao, Z. F.; Tian, D. Y.; Wang, D. L.; Yin, D. Q. Model of Hormesis and Its Toxicity Mechanism Based on Quorum Sensing: A Case Study on the Toxicity of Sulfonamides to *Photobacterium phosphoreum*. *Environ. Sci. Technol.* **2012**, *46* (14), 7746–7754.

(91) Boyd, E. M.; Killham, K.; Wright, J.; Rumford, S.; Hetheridge, M.; Cumming, R.; Meharg, A. A. Toxicity assessment of xenobiotic contaminated groundwater using lux modified *Pseudomonas fluorescens*. *Chemosphere* **1997**, *35* (9), 1967–1985.

(92) Bridgeman, J.; Baker, A.; Brown, D.; Boxall, J. B. Portable LED fluorescence instrumentation for the rapid assessment of potable water quality. *Sci. Total Environ.* **2015**, *524–525*, 338–46.

(93) Baker, A.; Ward, D.; Lieten, S. H.; Periera, R.; Simpson, E. C.; Slater, M. Measurement of protein-like fluorescence in river and waste water using a handheld spectrophotometer. *Water Res.* **2004**, *38* (12), 2934–2938.

(94) Bekins, B. A.; Cozzarelli, I. M. *Nonvolatile dissolved organic carbon and diesel range organics concentrations measured in 2016 at the USGS crude oil study site near Bemidji, Minnesota, USA*; U. S. Geological Survey data release 2017, <https://doi.org/10.5066/F7CN733T>.